

Effect of resistance-area product on spin-transfer switching in MgO-based magnetic tunnel junction memory cells

Z. M. Zeng,^{1,a)} P. Khalili Amiri,² G. Rowlands,³ H. Zhao,⁴ I. N. Krivorotov,³ J.-P. Wang,⁴ J. A. Katine,⁵ J. Langer,⁶ K. Galatsis,² K. L. Wang,² and H. W. Jiang¹

¹Department of Physics and Astronomy, University of California, Los Angeles, California 90095, USA

²Department of Electrical Engineering, University of California, Los Angeles, California 90095, USA

³Department of Physics and Astronomy, University of California, Irvine, California 92697, USA

⁴Department of Electrical and Computer Engineering, University of Minnesota, Minneapolis, Minnesota 55455, USA

⁵Hitachi Global Storage Technologies, San Jose, California 95135, USA

⁶Singulus Technologies, Kahl am Main 63796, Germany

(Received 24 November 2010; accepted 29 January 2011; published online 18 February 2011)

We use ultrafast current-induced switching measurements to study spin-transfer switching performance metrics, such as write energy per bit (E_W) and switching current density (J_c), as a function of resistance-area product (RA) (hence MgO thickness) in magnetic tunnel junction cells used for magnetoresistive random access memory (MRAM). E_W increases with RA , while J_c decreases with increasing RA for both switching directions. The results are discussed in terms of RA optimization for low write energy and current drive capability (hence density) of the MRAM cells. Switching times < 2 ns and write energies < 0.3 pJ are demonstrated for $135 \text{ nm} \times 65 \text{ nm}$ CoFeB/MgO/CoFeB devices. © 2011 American Institute of Physics. [doi:10.1063/1.3556615]

The spin-transfer torque (STT) effect, predicted by Slonczewski¹ and Berger,² shows great promise for enabling high density magnetoresistive random access memory (MRAM).^{3–5} In STT-MRAM bits, the spin torque can reverse the free layer magnetization if the current density is sufficient, resulting in spin-transfer-induced switching (STS). Remarkable progress in STS in giant magnetoresistive nanopillars⁶ and magnetic tunnel junctions (MTJs),⁷ particularly in MgO-based MTJs with large magnetoresistance (MR) ratio,^{8,9} has been achieved in recent years, but challenges remain to be overcome in terms of write current and write energy. High values for the critical current density required for STS, J_c , complicate the integration with complementary metal-oxide-semiconductor (CMOS), requiring larger transistors to increase the current drive capability. Moreover, present-day CMOS operates at speeds in the low gigahertz range, but J_c increases drastically with decreased switching time τ_p in the subnanosecond current pulse regime.^{10,11}

In this work, we study the effect of resistance-area (RA) product on the MTJ switching performance through ultrafast switching measurements. In our experiments, all conditions except MgO thickness of MTJ cells are controlled to be the same. We find that the write energy increases, while J_c decreases with increasing RA values, as described below.

MTJs with stacks of composition PtMn (15)/CoFe (2.5)/Ru (0.85)/CoFeB (2.4)/MgO (wedge: 0.8–1.0)/CoFeB (1.8) (thickness in nanometers) were deposited using a Singulus TIMARIS PVD system and annealed at 300 °C for 2.0 h in a magnetic field of 1 T. The films were subsequently patterned into ellipse-shaped pillars. In this letter, we show data from devices with $135 \text{ nm} \times 65 \text{ nm}$ nominal dimensions. Our previous works^{12,13} suggest that these MTJ cells have low J_c values and high thermal stability based on mea-

surements of the magnetic anisotropy field. Similar results were observed in devices with other sizes. Our experimental setup with short pulse capability is briefly described as follows. The MTJ cell is contacted by a one-port ground-signal-ground configuration microwave (40 GHz) probe. A short pulse and a dc are applied to the MTJ cell through a bias T and the resistance is recorded by a Keithley Instruments meter. Note that the real pulse voltage across the MTJ cells presented below was calibrated by considering the reflection and the loss L (in our system, $L \approx 0.0279$) in the cables and probe as $V_p = 2V_{in}(1-L)R/(R+50 \text{ } \Omega)$, where V_{in} is the input pulse amplitude and R is the resistance of the MTJ cell. During the pulse measurements, the polarity of the pulse and the initial orientation of free layer are fixed, while V_{in} and pulse duration τ are varied. In our convention, positive voltage corresponds to electrons traveling from the fixed to free layers favoring parallel state.

Figure 1(a) represents the RA (hence MgO thickness) dependence of the MR ratio. Note that the RA presented below corresponds to the parallel (P) state. It can be seen that the MR variation is relatively large when RA is below $4.0 \text{ } \Omega \mu\text{m}^2$, while MR becomes stable around 150% for $RA > 4.0 \text{ } \Omega \mu\text{m}^2$. Figure 1(b) depicts the field hysteresis loop for one typical MTJ cell with MR of 147% and RA of $4.9 \text{ } \Omega \mu\text{m}^2$. The coupling or interaction field (H_{int}) between the fixed and the free layer favors parallel alignment in our devices and is found to be $\sim 60\text{--}120$ Oe in our measured cells. We believe that the decrease in H_{int} with higher RA is due to reduced Néel coupling in the thicker barriers. The sharp resistance transition suggests that the free layer magnetization has an almost single-domain structure. Figure 1(c) shows the dc current-voltage (I - V) curves for the corresponding MTJ cell when the magnetizations of the fixed and free layers are aligned in the antiparallel (AP) and parallel (P) states as well as the switching state. In the dc switching loop, resistance shows abrupt changes at $+144 \text{ } \mu\text{A}$ (I_c^+) and

^{a)}Electronic mail: zhongming.zeng@gmail.com.

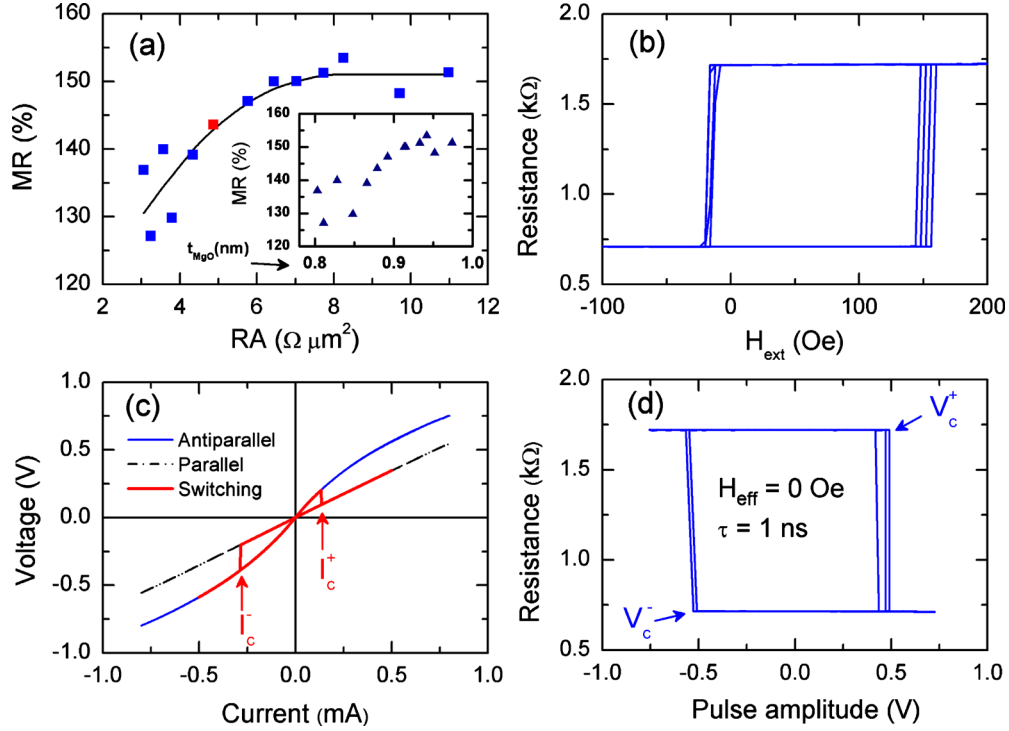


FIG. 1. (Color online) (a) MR ratio as a function of the resistance-area (RA) product; the inset is plotted as a function of the MgO thickness. The field hysteresis loop (b), current-voltage curves for AP, P, and switching states (c), and pulse voltage loop (d) in a typical MgO-MTJ cell with $RA=4.9 \Omega \mu\text{m}^2$. Here, MR is defined as $\text{MR}=100 \times (R_{\text{AP}}-R_{\text{P}})/R_{\text{P}}$ and the solid line in (a) is added for clarity.

$-293 \mu\text{A}(I_c^-)$, and the average switching current density $J_c=(I_c^+-I_c^-)/2A$ is $\sim 3 \text{ MA/cm}^2$ (A is cell area). Figure 1(d) shows the pulse voltage induced switching loops obtained at a 1 ns pulse. During the pulse measurement, the external field (H_{ext}) was applied along the easy-axis to cancel the coupling field, thus the total field $H_{\text{eff}}=H_{\text{int}}+H_{\text{ext}}=0$. The $J_c=(V_c^+-V_c^-)/(2RA)$ [where R is the resistance of MTJ cell obtained from dc I - V curve, as shown in Fig. 1(c)] at 1 ns pulse is $\sim 8 \text{ MA/cm}^2$, indicating that J_c increases drastically with decreased switching time τ_p .^{10,11}

In Figs. 2(a) and 2(b), the switching probabilities P_{sw} are

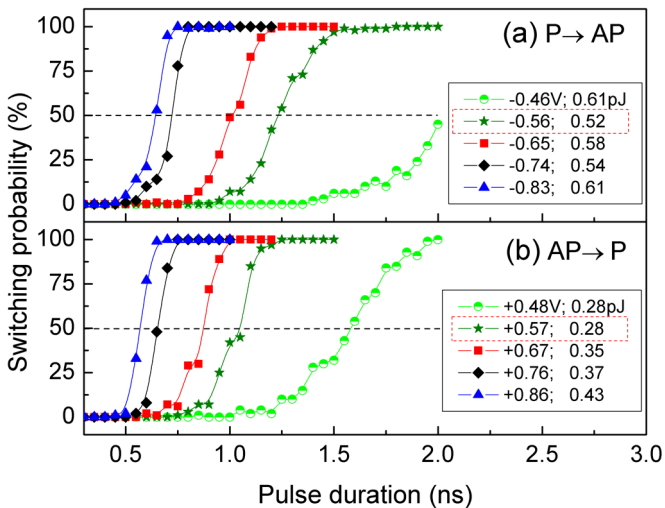


FIG. 2. (Color online) Switching probabilities (P_{sw}) as a function of the pulse width at various pulse amplitudes for AP \rightarrow P state (a) and P \rightarrow AP state (b) in the MgO-MTJ cell with $RA=4.9 \Omega \mu\text{m}^2$. The write energy per bit (E_w) is calculated at $P_{\text{sw}}=50\%$ (dashed line) and the dashed line box marks the E_w minima.

plotted as a function of pulse duration $\tau=0.3\text{--}2 \text{ ns}$ for P \rightarrow AP and AP \rightarrow P switching of the free layer for the corresponding MTJ cell at various pulse amplitudes. It can be seen that for both switching directions, the switching time τ_p decreases with increasing pulse amplitude. The energy per write for a given pulse amplitude can be estimated from

$$E_w = \frac{V_p^2 \tau_p}{R}, \quad (1)$$

where τ_p is the mean switching time corresponding to $P_{\text{sw}}=50\%$, as shown by the dashed line in Fig. 2. A minimum E_w for AP \rightarrow P(P \rightarrow AP) switching of 0.28 (0.52) pJ is obtained in this MTJ, as indicated in Fig. 2. Since our measurements are not in the thermal activation regime, the switching is dominated by angular momentum transfer rather than temperature, and according to an adiabatic precessional model,¹⁴ the switching time is given as

$$\tau_p = \tau_0 \ln\left(\frac{\pi/2}{\theta_0}\right) \bigg/ \left(\frac{V_p}{V_0} - 1\right), \quad (2)$$

where V_0 is the zero temperature instability voltage, τ_0 is the relaxation time, and θ_0 is the initial misalignment between spin polarization and the macrospin to be reversed. We found that $t_p(V_p)$ is consistent with our experiment, as shown in Fig. 3. By assuming $\theta_0=(k_B T/2E)^{1/2}=(1/2\Delta)^{1/2}=0.0745$ [$\Delta=90$ (Ref. 12)], $V_0=0.26(0.30) \text{ V}$ and $\tau_0=0.42(0.34) \text{ ns}$ for AP \rightarrow P(P \rightarrow AP) switching are obtained as fitting parameters.

Through measuring the switching probability P_{sw} of MTJ cells as mentioned above, we can get the energy per write for different RA values. Figure 4(a) shows the results of E_w as a function of RA . It can be clearly seen that E_w increases with increasing RA values for both switching direc-

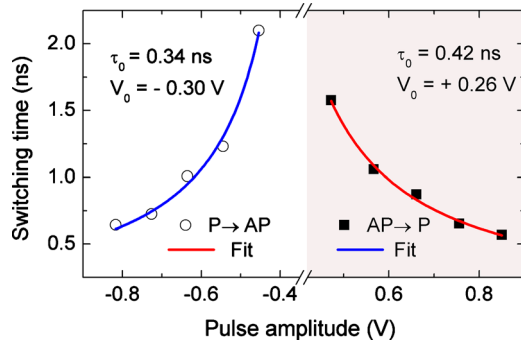


FIG. 3. (Color online) Pulse amplitude dependence of switching time for the MgO-MTJ cell with $RA=4.9 \Omega \mu\text{m}^2$.

tions. The increase in E_w is accompanied by an increase in the write voltage for larger RA values and is thus undesirable in terms of integration with low-power CMOS. Furthermore, write voltage (pulse amplitude) corresponding to the minimum E_w increases from ~ 0.35 V for $RA=3.0 \Omega \mu\text{m}^2$ to ~ 0.9 V for $RA=11.0 \Omega \mu\text{m}^2$ (not shown) because of the increase in the MTJ resistance with RA . The larger voltage across MTJ cell increases the probability of tunnel barrier

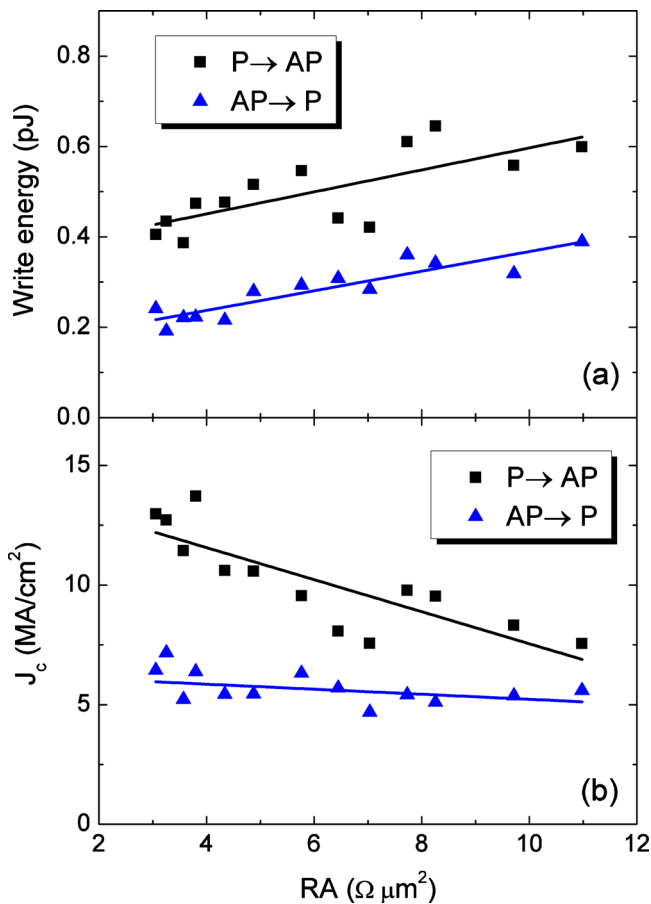


FIG. 4. (Color online) RA dependence of the write energy per bit E_w (a) and the switching current density J_c (b). The J_c values are calculated from pulse induced switching loop, as shown in Fig. 1(d); all data are collected at a pulse width of 1 ns. All solid lines are linear fits.

degradation and breakdown, lowering write endurance of the cell. RA optimization is thus essential for integration of the MTJ cell into a practical STT-MRAM circuit.

We also investigated the effect of RA on the switching current density J_c . The J_c values were determined by performing pulse induced switching loops for >20 times with 1 ns pulse, as shown in Fig. 1(d). In contrast to the write energy dependence of RA , J_c is found to decrease with increasing RA , as shown in Fig. 4(b). The reduction in J_c may originate from the decrease in effective damping due to spin pumping effect.¹⁵ Since this effective damping depends on the effective spin mixing conductance,^{16,17} high RA reduces the spin diffusion and spin mixing conductance.

In summary, we have investigated the effect of the resistance-area product on the spin-transfer switching in MgO-based MRAM cell. The write energy and write voltage are found to increase, while switching current density is reduced with increasing RA (i.e., MgO thickness). MTJ cells with switching times <2 ns and write energies <0.3 pJ are demonstrated with RA in the range of $\sim 4-8 \Omega \mu\text{m}^2$ and $MR > 140\%$.

We would like to acknowledge fruitful discussions with Y. Huai. This work was supported by the DARPA STT-RAM program (HR0011-09-C-0114) and the Nanoelectronics Research Initiative (NRI) through the Western Institute of Nanoelectronics (WIN).

¹J. C. Slonczewski, *J. Magn. Magn. Mater.* **159**, L1 (1996).

²L. Berger, *Phys. Rev. B* **54**, 9353 (1996).

³S. Ikeda, J. Hayakawa, Y. M. Lee, F. Matsukura, Y. Ohno, T. Hanyu, and H. Ohno, *IEEE Trans. Electron Devices* **54**, 991 (2007).

⁴S. Assefa, J. Nowak, J. Z. Sun, E. O'Sullivan, S. Kanakasabapathy, W. J. Gallagher, Y. Nagamine, K. Tsunekawa, D. D. Djayaprawira, and N. Watanabe, *J. Appl. Phys.* **102**, 063901 (2007).

⁵E. Chen, D. Apalkov, Z. Diao, A. Driskill-Smith, D. Druist, D. Lottis, V. Nikitin, X. Tang, S. Watts, S. Wang, S. A. Wolf, A. W. Ghosh, J. W. Lu, S. J. Poon, M. Stan, W. H. Butler, S. Gupta, C. K. A. Mewes, T. Mewes, and P. B. Visscher, *IEEE Trans. Magn.* **46**, 1873 (2010).

⁶J. A. Katine, F. J. Albert, R. A. Buhrman, E. B. Myers, and D. C. Ralph, *Phys. Rev. Lett.* **84**, 3149 (2000).

⁷Y. Huai, F. Albert, P. Nguyen, M. Pakala, and T. Valet, *Appl. Phys. Lett.* **84**, 3118 (2004).

⁸S. Yuasa, A. Fukushima, Y. Suzuki, and K. Ando, *Nature Mater.* **3**, 868 (2004).

⁹S. S. P. Parkin, C. Kaiser, A. Panchula, P. M. Rice, B. Hughes, M. Samant, and S.-H. Yang, *Nature Mater.* **3**, 862 (2004).

¹⁰T. Aoki, Y. Ando, D. Watanabe, M. Oogane, and T. Miyazaki, *J. Appl. Phys.* **103**, 103911 (2008).

¹¹Z. Diao, Z. Li, S. Wang, Y. Ding, A. Panchula, E. Chen, L. Wang, and Y. Huai, *J. Phys.: Condens. Matter* **19**, 165209 (2007).

¹²P. Khalili Amiri, Z. M. Zeng, P. Upadhyaya, G. Rowlands, H. Zhao, I. N. Krivorotov, J.-P. Wang, H. W. Jiang, J. A. Katine, J. Langer, K. Galatsis, and K. L. Wang, *IEEE Electron Device Lett.* **32**, 57 (2011).

¹³Z. M. Zeng, K. H. Cheung, H. W. Jiang, I. N. Krivorotov, J. A. Katine, V. Tiberkevich, and A. Slavin, *Phys. Rev. B* **82**, 100410(R) (2010).

¹⁴J. Z. Sun, *Phys. Rev. B* **62**, 570 (2000).

¹⁵Y. Tserkovnyak and A. Brataas, *Phys. Rev. B* **66**, 224403 (2002).

¹⁶Y. Huai, M. Pakala, Z. Diao, and Y. Ding, *Appl. Phys. Lett.* **87**, 222510 (2005).

¹⁷A. Brataas, Y. V. Nazarov, and G. E. W. Bauer, *Phys. Rev. Lett.* **84**, 2481 (2000).